Journal of Experimental Botany
doi:10.1093/jxb/ert460
This paper is available online free of all access charges (see http://jxb.oxfordjournals.org/open_access.html for further details)

Journal of Experimental Botany
www.jxb.oxfordjournals.org

RESEARCH PAPER

Deciphering early events involved in hyperosmotic stress-induced programmed cell death in tobacco BY-2 cells

Emanuela Monetti[1,2,3,*], Takashi Kadono[1,4,5,*], Daniel Tran[1,2], Elisa Azzarello[3], Delphine Arbelet-Bonnin[1,2], Bernadette Biligui[1,2], Joël Briand[1,2], Tomonori Kawano[3,4,6,7], Stefano Mancuso[3,6,7] and François Bouteau[1,2,3,6,†]

[1] Université Paris Diderot, Sorbonne Paris Cité, Institut des Energies de Demain (UMR8236), Paris, France
[2] Institut de Biologie des Plantes, Bât 630, 91405 Orsay, France
[3] LINV-DiSPAA, Department of Agri-Food and Environmental Science, University of Florence, Viale delle Idee 30, 50019 Sesto Fiorentino (FI), Italy
[4] Graduate School of Environmental Engineering, University of Kitakyushu 1-1, Hibikino, Wakamatsu-ku, Kitakyushu 808-0135, Japan
[5] Laboratory of Crop Science, Department of Plant Resources, Faculty of Agriculture, Kyushu University, 6-10-1 Hakozaki, Higashi-ku, Fukuoka 812–8581, Japan
[6] University of Florence LINV Kitakyushu Research Center (LINV@Kitakyushu), Kitakyushu, Japan
[7] Université Paris Diderot, Sorbonne Paris Cité, Paris Interdisciplinary Energy Research Institute (PIERI), Paris, France

* These authors contributed equally to this work.
† To whom correspondence should be addressed. E-mail: francois.bouteau@univ-paris-diderot.fr

Received 16 September 2013; Revised 22 November 2013; Accepted 26 November 2013

Abstract

Hyperosmotic stresses represent one of the major constraints that adversely affect plants growth, development, and productivity. In this study, the focus was on early responses to hyperosmotic stress- (NaCl and sorbitol) induced reactive oxygen species (ROS) generation, cytosolic Ca^{2+} concentration ($[Ca^{2+}]_{cyt}$) increase, ion fluxes, and mitochondrial potential variations, and on their links in pathways leading to programmed cell death (PCD). By using BY-2 tobacco cells, it was shown that both NaCl- and sorbitol-induced PCD seemed to be dependent on superoxide anion ($O_2^{\cdot -}$) generation by NADPH-oxidase. In the case of NaCl, an early influx of sodium through non-selective cation channels participates in the development of PCD through mitochondrial dysfunction and NADPH-oxidase-dependent $O_2^{\cdot -}$ generation. This supports the hypothesis of different pathways in NaCl- and sorbitol-induced cell death. Surprisingly, other shared early responses, such as $[Ca^{2+}]_{cyt}$ increase and singlet oxygen production, do not seem to be involved in PCD.

Key words: Calcium, hyperosmotic stress, mitochondria, NaCl, *Nicotiana tabacum*, non-selective cation channels, programmed cell death, reactive oxygen species.

Introduction

Salt stress is known to have severe effects on plant growth and development (Tester and Davenport, 2003). High salinity leads to ionic, osmotic, and oxidative stress in plants (Zhu, 2001) that may result in the induction of signalling events that lead to programmed cell death (PCD) in higher plants (Huh *et al.*, 2002; Lin *et al.*, 2006; Shabala, 2009; Wang *et al.*, 2010) and algae (Affenzeller *et al.*, 2009). Such PCD could be regarded as a salt adaptation mechanism (Huh *et al.*, 2002). Drought, which consists at least in part of a hyperosmotic stress, was also shown to induce PCD in plants (Duan *et al.*, 2010). PCD is an active cellular process that facilitates the removal of unwanted or damaged cells and is essential for cellular differentiation and tissue homeostasis (van Doorn *et al.*, 2011). PCD has effectively been proved to occur in response

to various abiotic stresses (Kadono *et al.*, 2010; van Doorn *et al.*, 2011). Different types of PCD with overlapping morphological and physiological hallmarks have been described in plants, which has led to a call for a detailed classification of cell death events (van Doorn, 2011; van Doorn *et al.*, 2011). Although the delineation between the different PCD types of sometimes remains difficult (van Doorn *et al.*, 2011), typical hallmarks of PCD in plants frequently include the fragmentation of the DNA by specific nucleases (DNA laddering), condensation and shrinkage of the cytoplasm, release of cytochrome *c* from mitochondria, elevation of the cytosolic calcium concentration ($[Ca^{2+}]_{cyt}$), generation of reactive oxygen species (ROS), and an activity increase of caspase-like enzymes (van Doorn, 2011; Tsiatsiani *et al.*, 2011).

Although early events reported in responses to ionic and non-ionic hyperosmotic stress such as a transient $[Ca^{2+}]_{cyt}$ increase (Xiong *et al.*, 2002; Donaldson *et al.*, 2004; Lin *et al.*, 2006; Kim *et al.*, 2007; Parre *et al.*, 2007; Ranf *et al.*, 2008), generation of ROS (Zhu, 2001; Xiong *et al.*, 2002; Lin *et al.*, 2006; Zhang *et al.* 2013), or up-regulation of protein kinases (Zhang *et al.*, 2013) seemed to be shared in plants, some other responses are specific to one of these stresses. Under saline conditions, Na^+ enters the cells through non-selective cation channels (NSCCs; Demidchik and Tester, 2002), depolarizing the plasma membrane (Chen *et al.*, 2007; Hua *et al.*, 2008; Shabala and Cuin, 2008; Pandolfi *et al.*, 2010; Wegner *et al.*, 2011). In contrast, isotonic mannitol or sorbitol solutions cause significant membrane hyperpolarization (Li and Delrot, 1987; Zingarelli *et al.*, 1999; Shabala *et al.*, 2000; Shabala and Lew, 2002). The DNA laddering, due to endonuclease release through permeable transition pores (PTPs) leading to mitochondria depolarization (Huh *et al.*, 2002; Lin *et al.*, 2006) occurred in NaCl- but not in sorbitol-stressed cells (Affenzeller *et al.*, 2009). Thus, although some common events are induced upon osmotic stress, multiple signal transduction pathways are involved in the response to ionic and non-ionic hyperosmotic treatments (Donaldson *et al.*, 2004; Parré *et al.*, 2007).

In this study, it was shown using Bright Yellow 2 (BY-2) cells that both ionic and non-ionic hyperosmotic stresses effectively induced early singlet oxygen ($^1O_2$) generation and an $^1O_2$-dependent influx of Ca^{2+}, which are not involved in PCD processes. The PCD observed in response to NaCl and sorbitol seemed to be dependent on delayed superoxide anion ($O_2^{\cdot-}$) generation by NADPH-oxidase, this last being linked to Na^+ influx through NSCCs and mitochondrial dysfunction only in the case of NaCl hyperosmotic stress.

Materials and methods

Cell culture conditions

Nicotiana tabacum L. BY-2 suspension cells were grown in Murashige and Skoog (MS) medium, pH 5.8 augmented with 30 g l^{-1} sucrose and 0.2 mg l^{-1} 2,4 D (Pauly *et al.*, 2001). Cells were maintained at 22 ± 2 °C, under continuous darkness and continuous shaking (gyratory shaker) at 120 rpm. Cell suspensions were subcultured weekly using a 1:15 dilution. All experiments were performed at 22 ± 2 °C using log-phase cells (6 d after subculture) maintained in their culture medium. Cell density was ~4×10^5 cells ml^{-1}.

Osmolality changes

The osmolality changes were systematically obtained by addition of 50 µl of sorbitol or NaCl from various stock solutions. For the measurement of extracellular medium osmolality changes after NaCl or sorbitol treatment, 100 µl of supernatant of cell suspensions treated with NaCl or sorbitol, were determined by the freezing depression method using an Automatic Micro-Osmometer Type 15 (Löser Messtechnik, Berlin, Germany).

Cell viability assays

Hyperosmosis-induced cell death in the cell suspension culture was determined by staining the dead cells with the vital dye Evans blue (0.005%, w/v) by mixing and incubating the cells and the dye for 10 min. Then stained cells were observed under a microscope. When appropriate, a 15 min pre-treatment with pharmacological effectors was done prior to NaCl or sorbitol exposure. Cells were counted under a microscope and cells that accumulated Evans blue were considered dead. At least 500 cells were counted for each independent treatment, and the procedure was repeated at least three times for each condition.

Monitoring of ROS production

The production of ROS was monitored by the chemiluminescence of the *Cypridina* luciferin analogue (CLA) as previously described (Kadono *et al.*, 2006, 2010). CLA is known to react mainly with $O_2^{\cdot-}$ and $^1O_2$ with light emission (Nakano, 1986), and allows measurement of extracellular ROS in plant cells (Tran *et al.*, 2013). Chemiluminescence from CLA was monitored using an FB12-Berthold luminometer (with a signal integrating time of 0.2 s). For data analysis, the luminescence ratio (L/L_{basal}) was calculated by dividing the intensity of CLA luminescence (L) by the luminescence intensity before treatment (L_{basal}). The ROS scavengers 1,2-dihydroxybenzene-3,5-disulphonic acid disodium salt (Tiron), 1,4-diazabicyclo[2.2.2]octane (DABCO), and salicylhydroxamic acid (SHAM) were added 5 min before NaCl and sorbitol treatment. Other inhibitors were added to the cell suspension 30 min before NaCl and sorbitol treatment.

Aequorin luminescence measurements

The $[Ca^{2+}]_{cyt}$ variations were recorded in a BY-2 cell suspension expressing the aequorin gene. Aequorin was reconstituted by overnight incubation in MS medium supplemented with 30 g l^{-1} sucrose and 2.5 µM native coelenterazine. Cell culture aliquots (500 µl) were transferred carefully into a luminometer tube, and the luminescence counts were recorded continuously at 0.2 s intervals with a luminometer. Treatments were performed by pipette injection of 50 µl of the effectors (NaCl or sorbitol). The residual aequorin was discharged by addition of 500 µl of a 1 M $CaCl_2$ solution dissolved in 100% methanol. The resulting luminescence was used to estimate the total amount of aequorin in each experiment. Calibration of calcium measurement was performed by using the equation: $pCa=0.332588(-\log k)+5.5593$, where k is a rate constant equal to luminescence counts per second divided by the total remaining counts (Knight *et al.*, 1996). The results are expressed in micromolar Ca^{2+} and correspond to the mean±SD of 3–5 independent experiments.

Voltage clamp measurements

Experiments were conducted on 6-day-old cells maintained in their culture medium to limit stress (main ions in MS medium 28 mM NO_3^-, 16 mM K^+). Individual cells were immobilized by a microfunnel (~50–80 µm outer diameter) and controlled by a micromanipulator (WR6-1, Narishige, Japan). Impalements were carried out with a piezoelectric micromanipulator (PCS-5000, Burleigh Inst., USA) in

a chamber (500 µl) made of Perspex. Voltage clamp measurements of whole-cell currents from intact cultured cells presenting a stable running membrane potential were carried out using the technique of the discontinuous single voltage clamp microelectrode (dSEVC; Finkel and Redman, 1984). In this technique, both current passing and voltage recording use the same microelectrode. Interactions between the two tasks are prevented by time-sharing techniques (sampling frequency 1.5–3 kHz). Microelectrodes were made from borosilicate capillary glass (Clark GC 150F, Clark Electromedical, Pangbourne Reading, UK) pulled on a vertical puller (Narishige PEII, Japan). Their tips were <1 µm diameter; they were filled with 600 mM KCl, and had electrical resistances between 20 MΩ and 50 MΩ with the culture medium. The capacity compensation of the microelectrode amplifier (Axoclamp 2A, Molecular Devices, Sunnyvale, CA, USA) was set to a subcritical level to produce the fastest electrode response. The relatively large size of the cells ensured a sufficiently high membrane time constant despite a relatively low input resistance (~40 MΩ). Specific software (pCLAMP 8) drives the voltage clamp amplifier. Voltage and current were simultaneously displayed on a dual input oscilloscope (Gould 1425, Gould Instruments Ltd, Hainault, UK), digitalized with a Digidata 1322A (Molecular Devices). In whole-cell current measurements, the membrane potential was held to the value of the resting membrane potential. Current recordings were obtained by hyperpolarizing pulses from –200 mV to +80 mV (20 mV, 2 s steps of current injection, 6 s of settling time). It was systematically checked that cells were correctly clamped by comparing the protocol voltage values with those really imposed. Only microelectrodes presenting a linear relationship were used.

Confocal microscopy

Confocal imaging was performed using an upright Leica Laser Scanning Confocal Microscope SP5 (Leica Microsystems, Germany) equipped with a ×63 oil immersion objective. To analyse the NaCl influx, the sodium indicator Sodium Green was used (Molecular Probes, USA). The BY-2 tobacco cells were pre-incubated for 15 min with an NSCC inhibitor and then incubated with 200 mM NaCl for 1 h. Sodium Green indicator (10 µM) was added to the solution 30 min after the beginning of the salt treatment. After incubation with NaCl and Sodium Green indicator, the BY-2 cells were washed with phosphate-buffered saline (PBS) buffer. The excitation wavelength was set at 514 nm, and the emission was detected at 530 ± 20 nm.

Mitochondrial membrane potential measurement

Six-day-old BY-2 suspension cells were collected and washed by filtration in a suspension buffer containing 50 mM HEPES, 0.5 mM $CaCl_2$, 0.5 mM K_2SO_4, and 10 mM glucose, pH 7.0 (Errakhi *et al.*, 2008). After treatment, cells were stained with the mitochondrial membrane potential probe JC-1 by incubating 2 ml of cell suspensions for 15 min (24 °C in the dark) with 2 µg ml^{-1} JC-1 (3 µM). JC-1 was dissolved and stored according to the manufacturer's instructions. Treated cells without prior washing were subjected to analysis using a Hitachi F-2000 fluorescence spectrophotometer. The excitation wavelength used was 500 nm. Fluorescence signals were collected using a band pass filter centred at 530 nm and 590 nm.

Chemicals

All chemical products were purchased from Sigma-Aldrich (Saint-Quentin Fallavier, France), except JC1 and Sodium Green indicator which were from Molecular Probes (Saint Aubin, France). Stock solution of diphenyleneiodonium chloride (DPI; 10 mM) was dissolved in dimethylsulphoxide (DMSO) in order to obtain a 0.01% final concentration of DMSO. This DMSO concentration did not induce any change in ROS or $[Ca^{2+}]_{cyt}$ levels (not shown). All other chemicals were dissolved in water.

Statistical analysis

Data were analysed by analysis of variance (ANOVA), and the mean separation was achieved by Newman and Keuls multiple range test. All numerical differences in the data were considered significantly different at the probability level of $P \leq 0.05$.

Results

Hyperosmotic changes induce cell death in N. tabacum *BY-2 suspension-cultured cells*

The impact of NaCl and sorbitol additions on osmolality changes in BY-2 medium was first evaluated and it was found that the concentrations of NaCl (200 mM) and sorbitol (400 mM) most frequently used in this study showed almost the same osmolality shifts (Table 1). These shifts in osmolality induced by 400 mM sorbitol or 200 mM NaCl led to the death of a part of the cell population, dead cells displaying large cell shrinkage (Fig. 1A), the hallmark of the PCD process (van Doorn, 2011). Cell death scoring at various concentrations of sorbitol and NaCl showed the time- and dose-dependent progression of death (Fig. 1B, C), half of the cells being dead after 4 h at 400 mM sorbitol and 200 mM NaCl. In order to confirm whether this cell death was due to an active process requiring active gene expression and cellular metabolism, BY-2 cell suspensions were treated with actinomycin D (AD), an inhibitor of RNA synthesis, or with cycloheximide (Chx), an inhibitor of protein synthesis, each at 20 mg ml^{-1}, 15 min prior to 200 mM NaCl or 400 mM sorbitol exposure. In both cases, AD and Chx significantly reduced cell death (Fig. 1D). These results indicated that this cell death required active cell metabolism, namely gene transcription and *de novo* protein synthesis. Taken together, these data showed that saline or non-saline hyperosmotic stress induced a rapid PCD of a part of the *N. tabacum* BY-2 suspension cell population.

The kinetics of some early events classically detected upon saline stress or drought, namely an increase in cytosolic Ca^{2+}, ion flux variations, ROS production, and mitochondrial membrane depolarization, were then followed, and it was checked how they could be involved in PCD induced by hyperosmotic stress.

Sorbitol- and NaCl-induced ROS generation

To study the effect of sorbitol on production of ROS in BY-2 cell suspension culture, the chemiluminescence of CLA, which indicates the generation of $O_2^{\cdot -}$ and $^1O_2$, was

Table 1. *Osmolality changes in the medium after treatment with NaCl and sorbitol*

	Medium	NaCl (mM)			Sorbitol (mM)		
		100	200	300	200	400	600
Osmolality (mosmol)	182	369	558	944	375	605	952

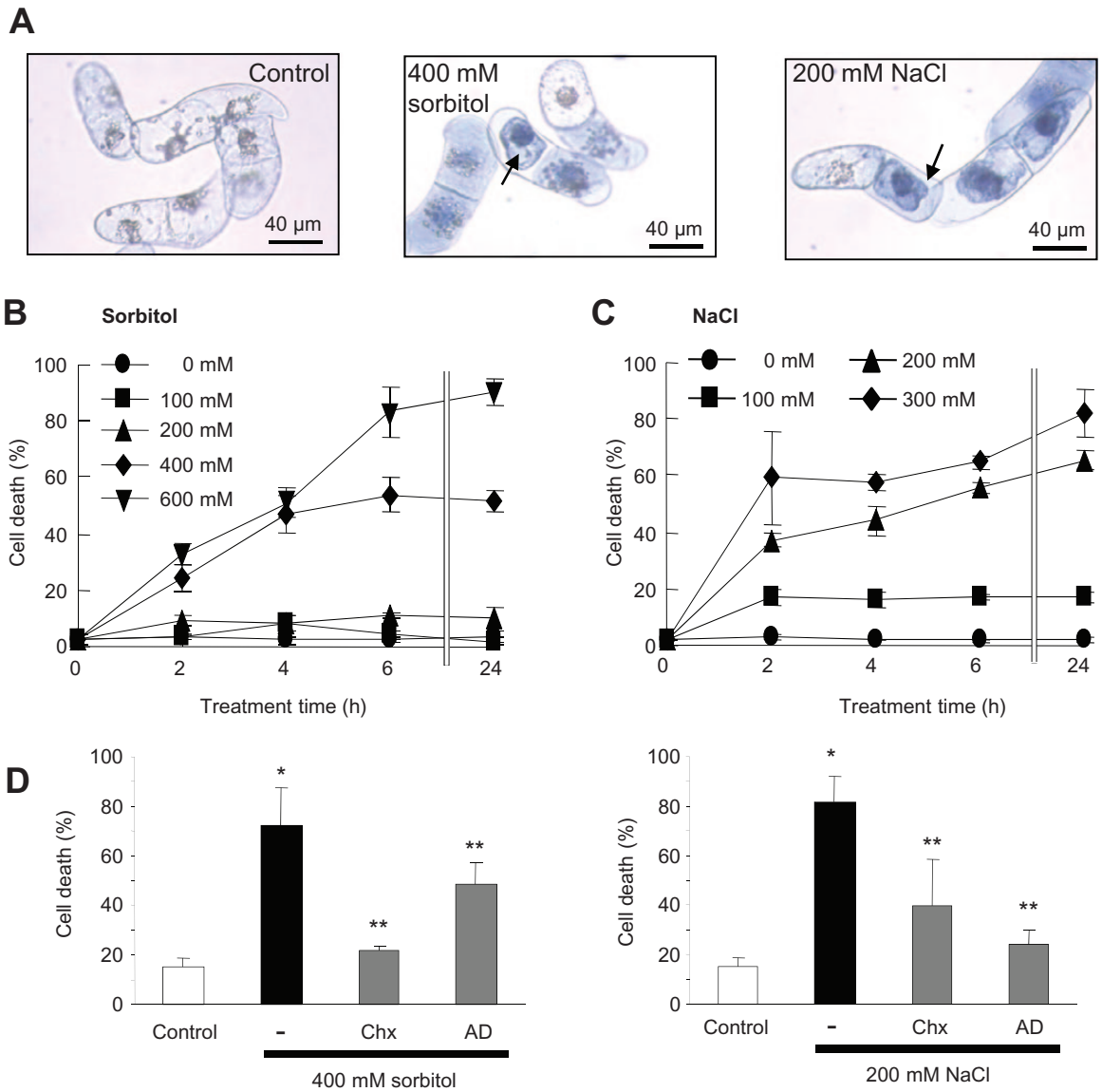

Fig. 1. NaCl- and sorbitol-induced cell death in tobacco BY-2 cells. (A) Light micrographs of BY-2 cultured cells stained with Evans blue 2 h after incubation with 400 mM sorbitol (centre) or 200 mM NaCl (right) compared with control cells maintained in their medium (left). Arrows indicate the cell shrinkage. (B) Effect of incubation time and concentration of sorbitol or NaCl on the extent of cell death. (C) Effect of pre-treatment with actinomycin D (AD; 20 µg ml^{-1}) or cycloheximide (Chx; 20 µg ml^{-1}) on sorbitol- and NaCl-induced cell death. Each data point and error bar reflect the mean and SD, respectively, of at least three independent replicates. *Significantly different from controls, $P < 0.05$; **significantly different from the NaC-l or sorbitol-treated cells, $P < 0.05$. (This figure is available in colour at *JXB* online.)

used. Addition of 400 mM sorbitol to BY-2 cell suspension culture resulted in transient production of ROS that reaches the maximal level immediately after treatment (Fig. 2A). This sorbitol-induced ROS generation was dose dependent (Fig. 2B) and could be blocked using DABCO, an $^1O_2$ scavenger, but not Tiron, an $O_2^{\cdot -}$ scavenger (Fig. 2A, C). Addition of 200 mM NaCl to BY-2 cell suspension culture also resulted in transient production of ROS that reaches the maximal level immediately after NaCl treatment (Fig. 2D, E). In the case of sorbitol, only DABCO was able to decrease the NaCl-induced CLA chemiluminescence (Fig. 2D, F). Thus, in both cases the early increase in CLA chemiluminescence seemed to be dependent on $^1O_2$ generation but not on $O_2^{\cdot -}$ generation. SHAM, an inhibitor of peroxidase (POX) (Kawano *et al.*, 1998; Hossain *et al.*, 2013), which could be responsible for extracellular $^1O_2$ generation (Kawano *et al.*, 1998; Kanofsky, 2000; Guo *et al.*, 2009), was thus used. Pre-treatment of the BY-2 cell suspension culture with 5 mM SHAM only slightly reduced the increase in CLA chemiluminescence induced by 400 mM sorbitol (Fig. 2C) but significantly reduced that induced by 200 mM NaCl (Fig. 2F). This suggests the involvement of POX, at least in NaCl-induced $^1O_2$ generation.

The impact of ROS pharmacology on NaCl- and sorbitol-induced PCD (Fig. 1) was further checked. DABCO, the $^1O_2$ scavenger, failed to decrease sorbitol- (400 mM) and

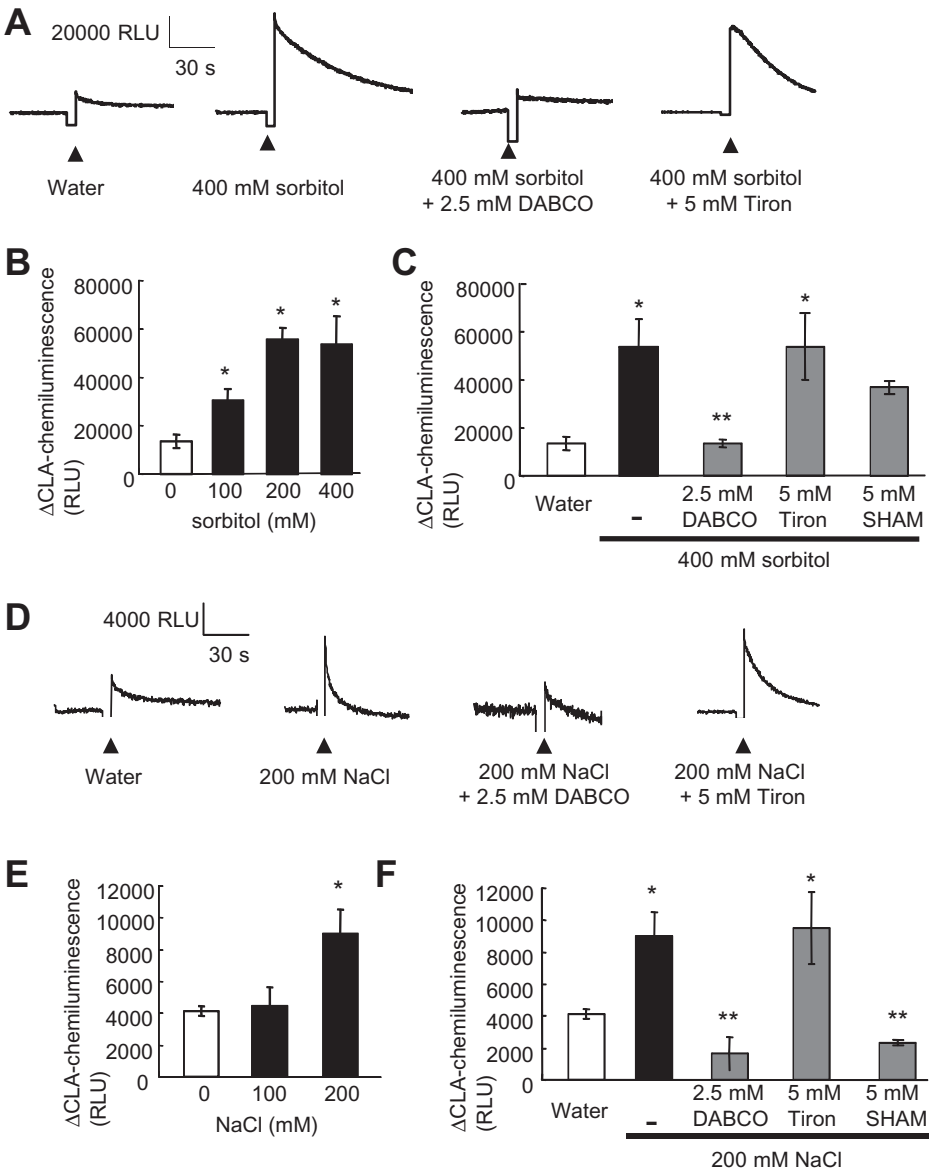

Fig. 2. Induction of rapid ROS generation in tobacco BY-2 cells by sorbitol or NaCl. (A) Typical kinetics of the sorbitol-induced increase in CLA chemiluminescence reflecting the production ROS and modulation by ROS scavengers. (B) Effect of the concentration of sorbitol on ROS generation. (C) Modulation of sorbitol-induced ROS generation by DABCO, a scavenger of singlet oxygen, Tiron, a scavenger of the superoxide anion, or salicylhydroxamic acid (SHAM), an inhibitor of peroxidase. (D) Typical kinetics of the NaCl-induced increase in CLA chemiluminescence and modulation by ROS scavengers. (E) Effect of the concentration of NaCl on ROS generation. (F) Modulation of NaCl-induced ROS generation by DABCO, Tiron, or SHAM. Each data point and error bar reflect the mean and SD, respectively (n=5). *Significantly different from controls, $P < 0.05$; **significantly different from the NaCl- or sorbitol-treated cells, $P < 0.05$.

NaCl- (200 mM) induced cell death and even increased NaCl-induced cell death after 2 h of treatment (Fig. 3A, B). For Tiron, the $O_2^{\cdot -}$ scavenger, there was no effect after 2 h but a decrease in cell death could be observed after 4 h treatment with NaCl (Fig. 3B). Thus, the hyperosmotic stress-induced cell death seemed not to be dependent on $^1O_2$ generation but on $O_2^{\cdot -}$ generation. Thus a possible delayed $O_2^{\cdot -}$ generation after treatment with 400 mM sorbitol or 200 mM NaCl was searched for. After such hyperosmotic stress, increases in CLA chemiluminescence could be detected (Fig. 3C). In both cases of CLA chemiluminescence increases, the maximum chemiluminescence levels were reached after 1 h and then decreased to the control level after 4 h, the decrease being more rapid upon NaCl treatement (Fig. 3C). It is noteworthy that these increases occurred before cell death reached the plateau level (Fig. 1B, C). These increases in CLA chemiluminescence could be inhibited by pre-treatment with Tiron, but also with 10 μM DPI, an inhibitor of NADPH-oxidase (Fig. 3D), suggesting that the generation $O_2^{\cdot -}$ through enhancement of NADPH-oxidase activity was involved in the delayed ROS generation after treatment with sorbitol and NaCl (Fig. 3C). In agreement with this, 10 μM DPI could also significantly reduce both sorbitol- and NaCl-induced cell death after 4 h (Fig. 3A, B).

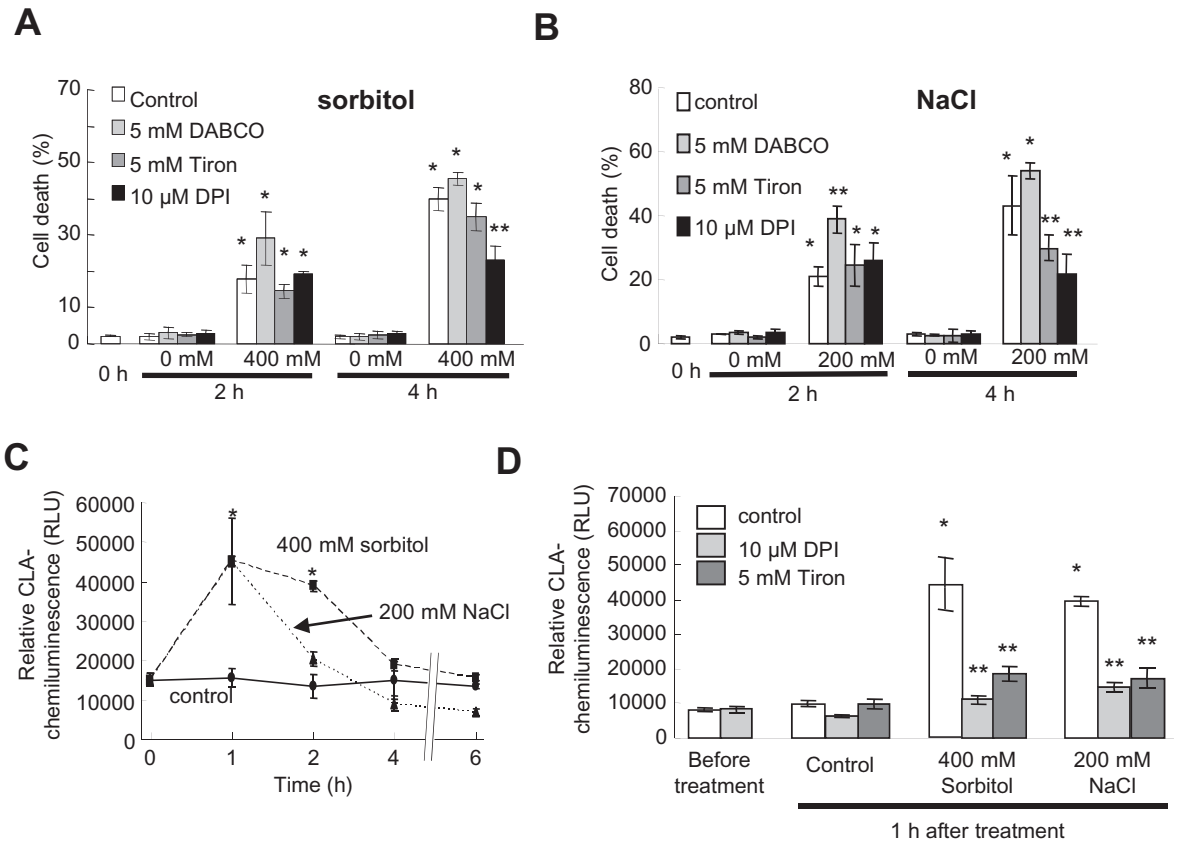

Fig. 3. Effects of ROS scavengers on NaCl- or sorbitol-induced cell death in BY-2 cells. (A) Effect of Tiron, DABCO, or DPI, an NADPH-oxidase inhibitor, on cell death induced by 400 mM sorbitol after 2 h or 4 h treatment. (B) Effect of Tiron, DABCO, or DPI on cell death induced by 200 mM NaCl after 2 h or 4 h treatment. (C) Time course of CLA chemiluminescence during 6 h treatment with 400 mM sorbitol or 200 mM NaCl. (D) Inhibition of sorbitol and NaCl-induced delayed ROS generation by Tiron or DPI. Each data point and error bar reflect the mean and SD, respectively (n=3). *Significantly different from controls, $P < 0.05$; **significantly different from the NaCl- or sorbitol-treated cells, $P < 0.05$.

Sorbitol and NaCl induce a rapid change in $[Ca^{2+}]_{cyt}$

The changes in $[Ca^{2+}]_{cyt}$ were monitored by the Ca^{2+}-dependent emission of blue light from aequorin (Knight *et al.*, 1996). Treatment of BY-2 cells with sorbitol (400 mM) resulted in a rapid transient increase in aequorin luminescence (Fig. 4A) reflecting an increase in $[Ca^{2+}]_{cyt}$ of 0.145 ± 0.035 μM (n=23). This increase could be inhibited by the presence of Ca^{2+} channel blockers, $LaCl_3$ and $GdCl_3$, when Ca^{2+} internal store inhibitors (U73122 and dantrolene, Meimoun *et al.*, 2009) showed no significant inhibitory effects (Fig. 4B), indicating that the sorbitol-induced increase in $[Ca^{2+}]_{cyt}$ is mainly due to influx of Ca^{2+} across the plasma membrane through Ca^{2+} channels. As the generation of $^1O_2$ by sorbitol occurred immediately upon hyperosmotic stress (Fig. 2A), the effect of ROS pharmacology on the sorbitol-induced increase in $[Ca^{2+}]_{cyt}$ was further tested. The $^1O_2$ scavenger DABCO strongly reduced the $[Ca^{2+}]_{cyt}$ increase compared with that in control cells; the POX inhibitor SHAM showed lower efficiency, while no differences were seen with the $O_2^{\cdot -}$ scavenger Tiron (Fig. 4A, C). These results strongly suggested that sorbitol-induced Ca^{2+} uptake through Ca^{2+} channels occurs downstream of the sorbitol-induced $^1O_2$ generation.

In the same way, treatment of BY-2 cells with NaCl (200 mM) resulted in a transient increase in aequorin luminescence (Fig. 4D), reflecting an increase in $[Ca^{2+}]_{cyt}$ of 0.217 ± 0.059 μM (n=23). As for sorbitol, inhibitors of Ca^{2+} release from intracellular organelles (U73122 and dantrolene) failed to suppress the NaCl-induced increase in $[Ca^{2+}]_{cyt}$ whereas Ca^{2+} channel blockers $LaCl_3$ and $GdCl_3$ were efficient at reducing the NaCl-induced increase in $[Ca^{2+}]_{cyt}$ (Fig. 4E). In a similar manner to what was observed for sorbitol, this increase was shown to be inhibited by the presence of DABCO (Fig. 4F) but less efficiently by SHAM, whereas Tiron seemed even to increase this Ca^{2+} influx (Fig. 4D, F). The effect of the Ca^{2+} channel inhibitor La^{3+} on NaCl- and sorbitol-induced cell death in BY-2 suspension-cultured cells was then studied. Lanthanum (500 μM) failed to decrease sorbitol- (400 mM) and NaCl- (200 mM) induced cell death and even increases this cell death after 2 h of treatment (Fig. 4G), as observed for DABCO with NaCl (Fig. 3B). These data are in agreement with the link observed between the immediate $^1O_2$ generation inducing an influx of Ca^{2+} upon sorbitol or NaCl stress and further suggest that these early induced events are not involved in a pathway leading to PCD.

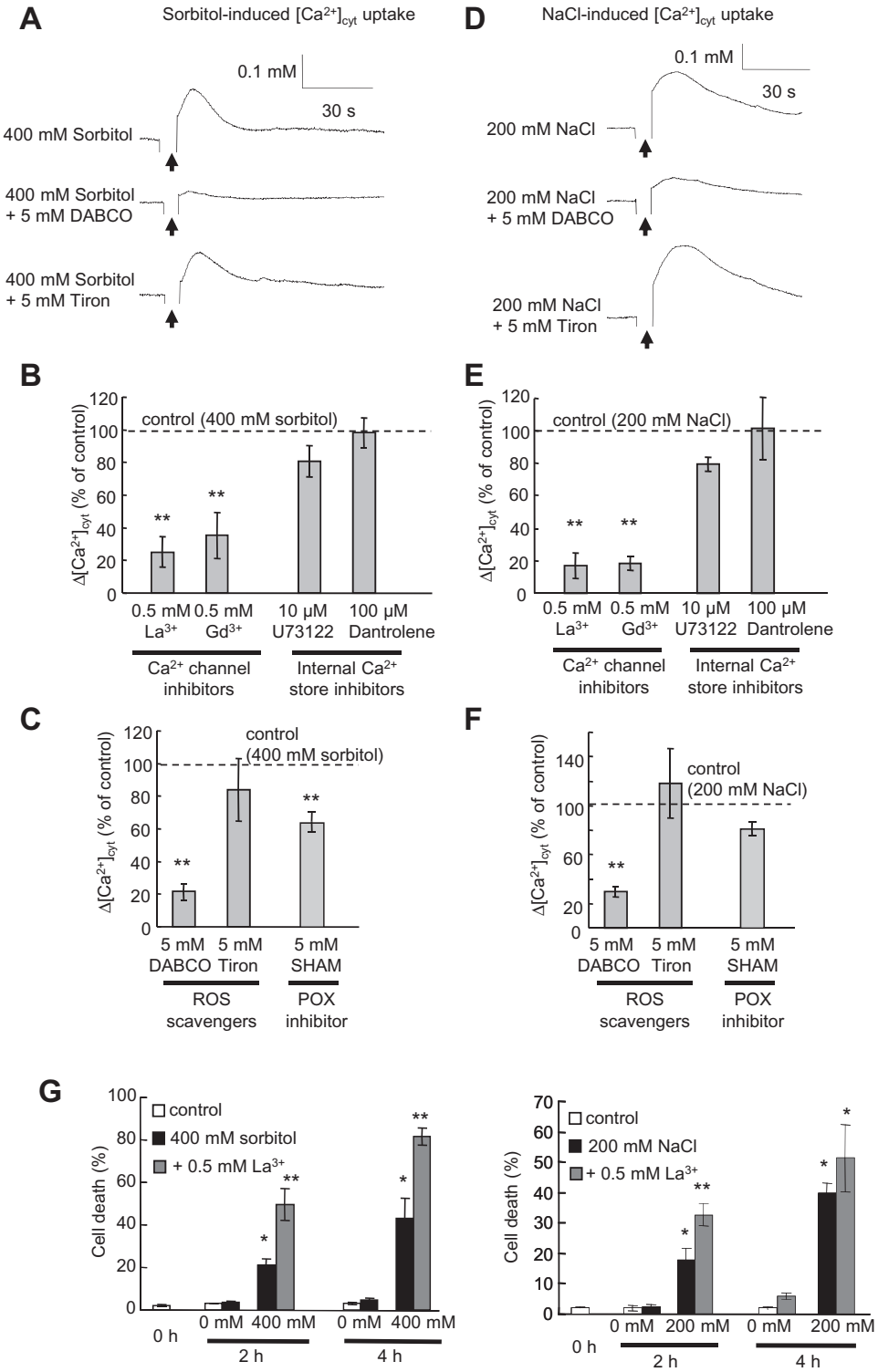

Fig. 4. Induction of $[Ca^{2+}]_{cyt}$ increase in aequorin-expressing tobacco BY-2 cells by sorbitol or NaCl. (A) Typical kinetics of sorbitol-induced increase in $[Ca^{2+}]_{cyt}$ and modulation by ROS scavengers. (B) Modulation of sorbitol-induced $[Ca^{2+}]_{cyt}$ increase by the calcium channel blockers La^{3+} or Gd^{3+} (500 μM each) and the internal stock release inhibitors U73122 (100 μM) and dantrolene (10 μM). (C) Modulation of sorbitol-induced $[Ca^{2+}]_{cyt}$ increase by DABCO, a scavenger of singlet oxygen, Tiron, a scavenger of anion superoxide, or salicylhydroxamic acid (SHAM), an inhibitor of peroxidase. (D) Typical kinetics of the NaCl-induced increase in $[Ca^{2+}]_{cyt}$ and modulation by ROS scavengers. (E) Modulation of the NaCl-induced $[Ca^{2+}]_{cyt}$ increase by La^{3+}, Gd^{3+} (500 μM each), U73122 (100 μM), or dantrolene (10 μM). (F) Modulation of NaCl-induced $[Ca^{2+}]_{cyt}$ increase by DABCO, Tiron, or SHAM. (G) Effect of La^{3+} on cell death induced by 200 mM NaCl (left) or 400 mM sorbitol (right) after 2 h or 4 h treatment. Each data point and error bar reflect the mean and SD, respectively (n=5). *Significantly different from controls, $P < 0.05$; **significantly different from the NaCl- or sorbitol-treated cells, $P < 0.05$.

Hyperosmotic constraints induce change in membrane potential and ion channel activities

Saline and non-saline hyperosmotic stresses are well known to modify the plasma membrane potential (V_m) of cells (Teodoro *et al.*, 1998; Zingarelli *et al.*, 1999; Shabala and Cuin, 2008; Wegner *et al.*, 2011). By using an electrophysiological technique (dSEVC), the impact of NaCl and sorbitol on BY-2 cultured cell membrane potential was investigated. In control conditions in culture medium, the V_m of BY-2 cells was –21.1 ± 2.2 mV (n=15). In MS medium, the main ions are 16 mM K^+ and 28 mM NO_3^-; thus the equilibrium potential estimated for K^+, E_K, is about –46 mV ($[K^+]_{out}$=16 mM with $[K^+]_{in}$ estimated at 100 mM). The equilibrium potential estimated for NO_3^- is about –25 mV ($[NO_3^-]_{out}$=28 mM with $[NO_3^-]_{in}$ estimated at 5 mM). As previously observed with cultured cells of *Arabidopsis thaliana* (Kadono *et al.*, 2010; Tran *et al.*, 2013) or tobacco (Gauthier *et al.*, 2007), the occurrence of anion currents in most of the BY-2 cells in their culture medium could explain the mean polarization of around –20 mV recorded in control and non-stressed conditions. The mean control value of these currents at –200 mV and after 1.8 s of voltage pulse was –1.12 ± 0.2 nA (n=11). These currents were shown to be sensitive to structurally unrelated anion channel inhibitors, 9-anthracene carboxylic acid (9-AC) and glibenclamide (gli) (Supplementary Fig. S1 available at *JXB* online), reinforcing the hypothesis of an anionic nature for these currents. Addition of NaCl to suspension cultures resulted in a significant membrane depolarization (Fig. 5A) when sorbitol induced a hyperpolarization of the cells (Fig. 5A), clearly indicating a difference between saline and non-saline hyperosmotic stress. The sorbitol-induced hyperpolarization was correlated with a decrease in anion current (Fig. 5B) when the NaCl-induced depolarization was correlated with a large increase in whole-cell ion current (Fig. 5B). The positive shifts of the reversal potential of the current upon addition of NaCl are in accordance with a current carried by Na^+.

The influx of Na^+ through the plasma membrane by NSCCs was the most probable reason for the cell depolarization (Demidchick *et al.*, 2002*a*, *b*), this Na^+ uptake was further checked using the Na^+-sensitive fluorescent probe Sodium Green (Wegner *et al.*, 2011). An accumulation of fluorescence in the cytoplasm of the cells could be observed after

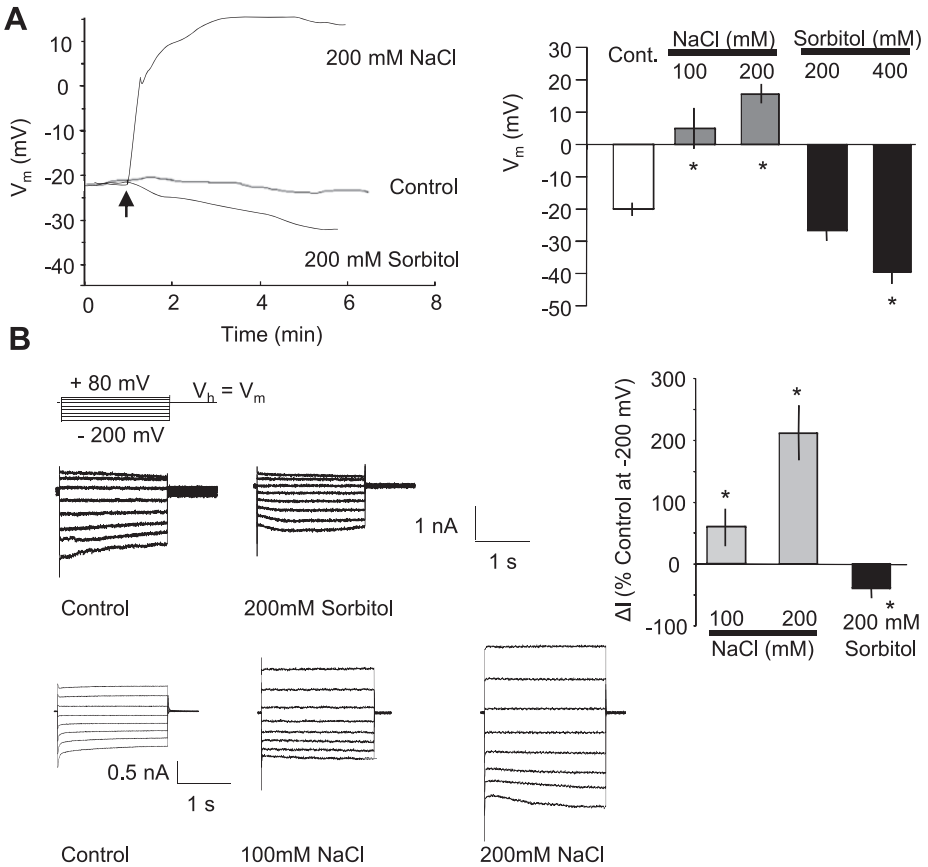

Fig. 5. (A) Typical modulation of BY-2 cultured cell plasma membrane (PM) potential variations observed in response to NaCl or sorbitol. (B) Mean values of PM potentials recorded a few minutes after treatment with NaCl (100 mM or 200 mM) or sorbitol (200 mM or 400 mM). (C) Typical changes in whole-cell current profiles after treatments with sorbitol (up) or NaCl (down). The protocol was as illustrated; the holding potential (V_h) was V_m. (D) Mean values of whole-cell current variations (recorded at –200 mV and 1.8 s) after treatment with NaCl or sorbitol. Current variations are given as a percentage of the control level before treatments. The data correspond to means of at least five independent replicates, and error bars correspond to the SD. *Significantly different from controls, $P < 0.05$.

1 h treatment with 200 mM NaCl (Fig. 6A). This fluorescence could be reduced by using pre-treatments with inhibitors of NSCC, 5 mM tetraethylammonium chloride (TEA^+) or 1 mM quinine (Demidchick *et al.*, 2002*a*) (Fig. 6A). Addition of 1 mM quinine or 5 mM TEA^+ also allowed reduction of the NaCl-induced increase in currents (Fig. 6B, C) in BY-2 cells, as did verapamil (100 µM), another potent inhibitor of NSCCs (Demidchick *et al.*, 2002*a*). The impact of these NSCC blockers on the extent of NaCl-induced cell death was thus further tested. The NSCC blockers were efficient at reducing the cell death induced by 200 mM NaCl (Fig. 6D), suggesting that NSCC activation is related to the NaCl-induced cell death. As this cell death was also dependent on a delayed $O_2^{\cdot -}$ generation by NADPH-oxidase (Fig. 3), the effect of the earliest activation of NSCCs by NaCl on this delayed ROS production was also checked. As for cell death, the NSCC blockers were efficient at reducing this NaCl-dependent delayed ROS production (Fig. 6E), suggesting that NaCl influx participates in the $O_2^{\cdot -}$ generation. Interestingly, the calcium channel blocker La^{3+} did not allow the delayed ROS generation to be decreased, confirming the hypothesis of the induction of different pathways in response to NaCl stress.

Mitochondrial depolarization is involved in NaCl- but not sorbitol-induced cell death

The role of mitochondria is well recognized in salinity tolerance (Jacoby *et al.*, 2011), and dysfunction of mitochondria, leading to cytochrome *c* release upon salt stress, was shown to induce PCD in *Thellungiella halophila* suspension-cultured cells (Wang *et al.*, 2010). Mitochondria are effectively pivotal in controlling cell life and PCD, through complex mechanisms that culminate in opening of PTPs leading to mitochondrial membrane potential ($\Delta\Psi_m$) loss (Vianello *et al.*, 2007). It was thus checked whether NaCl and sorbitol lead to a decrease in $\Delta\Psi_m$ in the present model. In untreated cells, the JC-1 fluorescence ratio of mitochondria displaying a high $\Delta\Psi_m$ versus mitochondria presenting a low $\Delta\Psi_m$ was greatly superior to 1 (Fig. 7A). This ratio decreased in a time-dependent manner upon addition of NaCl (200 mM), indicating that NaCl induced a significant decrease of $\Delta\Psi_m$ in some mitochondria when sorbitol (400 mM) induced an increase of $\Delta\Psi_m$ during the first 30 min, the ratio reaching the control value after 2 h (Fig. 7A). Since a mitochondrial $\Delta\Psi_m$ decrease during cell death was reported to be due to the formation of the mitochondrial PTPs (Vianello *et al.*, 2007), the effect of cyclosporin A (CsA), an inhibitor of PTPs, was tested on NaCl-induced mitochondrial depolarization. A pre-treatment with CsA significantly reduced the NaCl-induced mitochondrial depolarization after 15 min (Fig. 7B), indicating that mitochondrial PTPs were involved in NaCl-induced mitochondrial depolarization. Moreover, pre-treatment with CsA significantly inhibited NaCl-induced cell death (Fig. 7C), indicating that PTP formation could participate in NaCl-induced cell death. As the activation of NSCCs occurs rapidly upon NaCl stress (Fig. 5A) and is involved in ROS generation (Fig. 6E), the impact of sodium influx on $\Delta\Psi_m$ was investigated by using NSCC inhibitors. A significant reduction of NaCl-induced mitochondrial depolarization was observed after pre-treatment with verapamil (Fig. 7B). These data show that (i) two different pathways could be involved in the hyperosmotic stress-induced cell death; and (ii) the ROS generation dependent on Na^+ influx could participate in the decrease in $\Delta\Psi_m$ during NaCl-induced cell death.

Discussion

As expected from previous studies (Huh, 2002; Wang, 2010), the death of a part of the BY-2 cell population characterized by large cell shrinkage, a hallmark of the PCD process (van Doorn, 2011), was observed in response to NaCl-induced hyperosmotic stress. The extent of cell death was time and dose dependent, reaching about half of the population in 4 h with 200 mM NaCl. In order to check whether this cell death was due to an active mechanism requiring active gene expression and cellular metabolism, BY-2 cell suspensions were treated with AD, an inhibitor of RNA synthesis, or with Chx, an inhibitor of protein synthesis, prior to NaCl exposure. AD and Chx significantly reduced the NaCl-induced cell death. These results indicated that this cell death required active cell metabolism, namely gene transcription and *de novo* protein synthesis. The same behavior, namely time- and dose-dependent cell death characterized by cell shrinkage and requiring active metabolism using iso-osmotic concentrations of sorbitol, was observed here. This suggests that non-ionic hyperosmotic stress, like ionic hyperosmotic stress, could induce PCD in BY-2 cells as previously observed in various animal cell lines (Murata *et al.*, 2002; Galvez *et al.*, 2003; Niswander and Dokas, 2007). It was then checked whether some early events classically detected during hyperosmotic stress responses and PCD in plant could be involved in this cell death, namely ROS production, an increase in cytosolic Ca^{2+}, ion flux variations, and mitochondrial membrane depolarization.

The earliest response observed after exposure of BY-2 cells to NaCl was an immediate peak of ROS. Addition of Tiron (a scavenger of $O_2^{\cdot -}$) did not significantly reduce NaCl-induced ROS generation, whereas DABCO (a scavenger of $^1O_2$) avoided this production. Although $^1O_2$ formation is likely to occur during the exposure to high light intensities (Krieger-Liszkay, 2004), it was also found that different enzymes including POXs could produce extracellular $^1O_2$ in animals (Kanofsky, 2000; Stief, 2003; Tarr and Valenzeno, 2003) and in plant cells (Kawano *et al.*, 1998; Guo *et al.*, 2009). As the studied cultured cells were non-photosynthetic, the POX inhibitor SHAM was further tested (Kawano *et al.*, 1998; Hossain *et al.*, 2013), and this could reduce the early NaCl-induced ROS generation effectively. Thus, it would appear that these early transient $^1O_2$ generations are not specific to ionic or non-ionic hyperosmotic stress.

In the case of both NaCl and sorbitol treatments, rapid transient $[Ca^{2+}]_{cyt}$ increases in BY-2 cells were observed, as previously described in various models (Knight *et al.*, 1997; Donaldson *et al.*, 2004; Lin *et al.*, 2006; Parre *et al.*, 2007; Ranf *et al.*, 2008). In BY-2 cells, these $[Ca^{2+}]_{cyt}$ increases were inhibited by the calcium channel blockers La^{3+} and

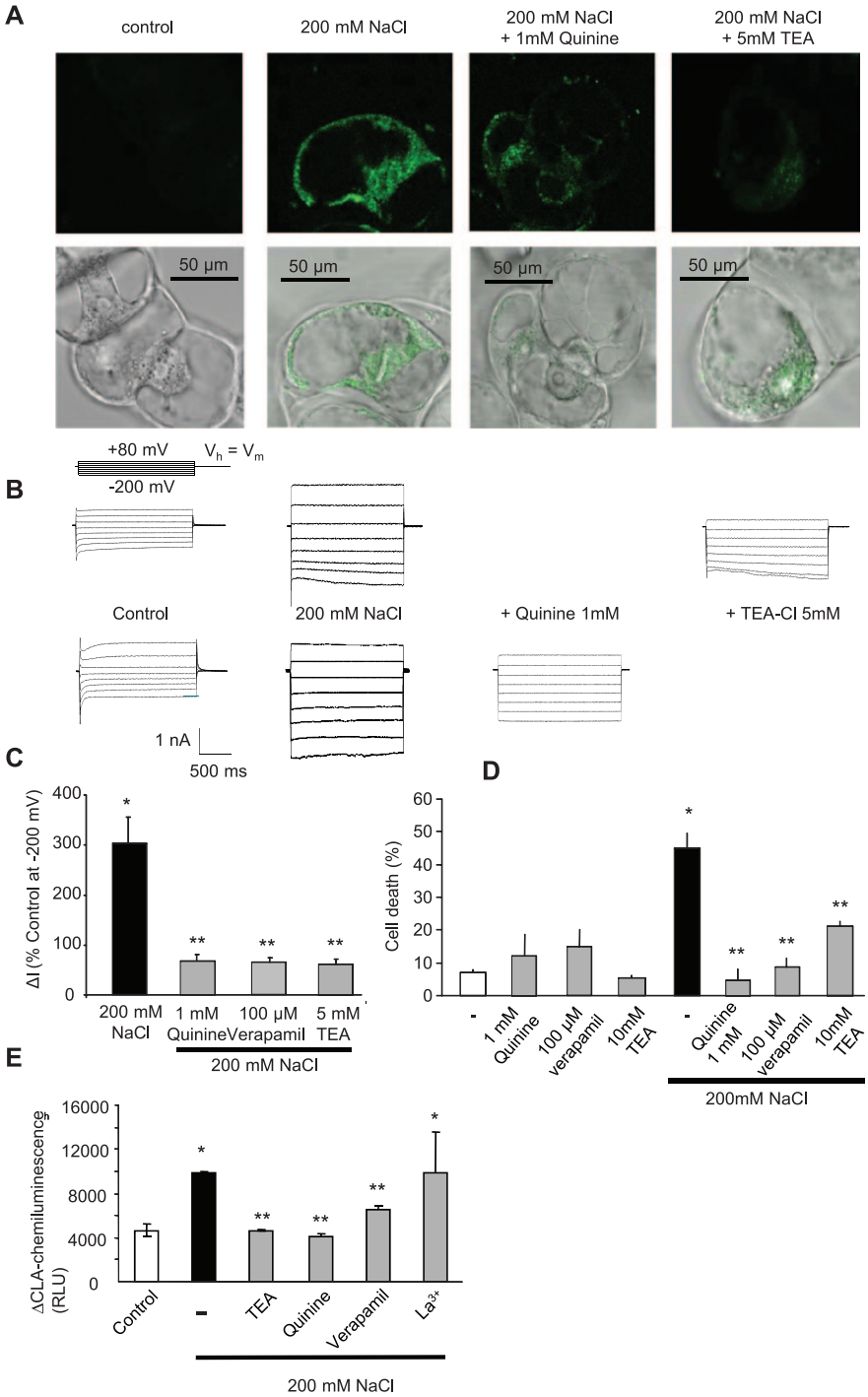

Fig. 6. (A) Confocal imaging of NaCl accumulation in BY-2 cells after 1 h treatment with 200 mM NaCl using the Sodium Green fluorescent probe (left). Decrease in fluorescence in cells pre-treated with quinine (1 mM) or TEA^+ (5 mM), blockers of non-selective cation channels (NSCCs), prior to NaCl treatment (right). Corresponding bright field images are shown on the line below. Each image is representative of symptoms observed in at least three independent experiments. (B) Variations of whole-cell currents recorded before and after addition of 200 mM NaCl and subsequent addition of 1 mM quinine or 5 mM TEA^+. The protocol was as illustrated; the holding potential (V_h) was V_m. (C) Mean values of whole-cell current variations (recorded at –200 mV and 1.8 s) after treatment with 200 mM NaCl with or without the NSCC blockers quinine (1 mM), TEA^+ (5 mM), or verapamil (200 µM). Current variations are given as a percentage of the control level before treatments. The data correspond to means of at least five independent replicates, and error bars correspond to the SD. (D) Effect of pre-treatments with the NSCC blockers on NaCl-induced cell death. The data correspond to means of at least four independent replicates, and error bars correspond to the SD. (E) Effect of pre-treatments with the NSCC blockers or with La^{3+} (500 µM) on NaCl-induced delayed ROS generation and cell death. The data correspond to means of at least five independent replicates, and error bars correspond to the SD. *Significantly different from controls, $P < 0.05$; **significantly different from the NaCl- or sorbitol-treated cells, $P < 0.05$. (This figure is available in colour at *JXB* online.)

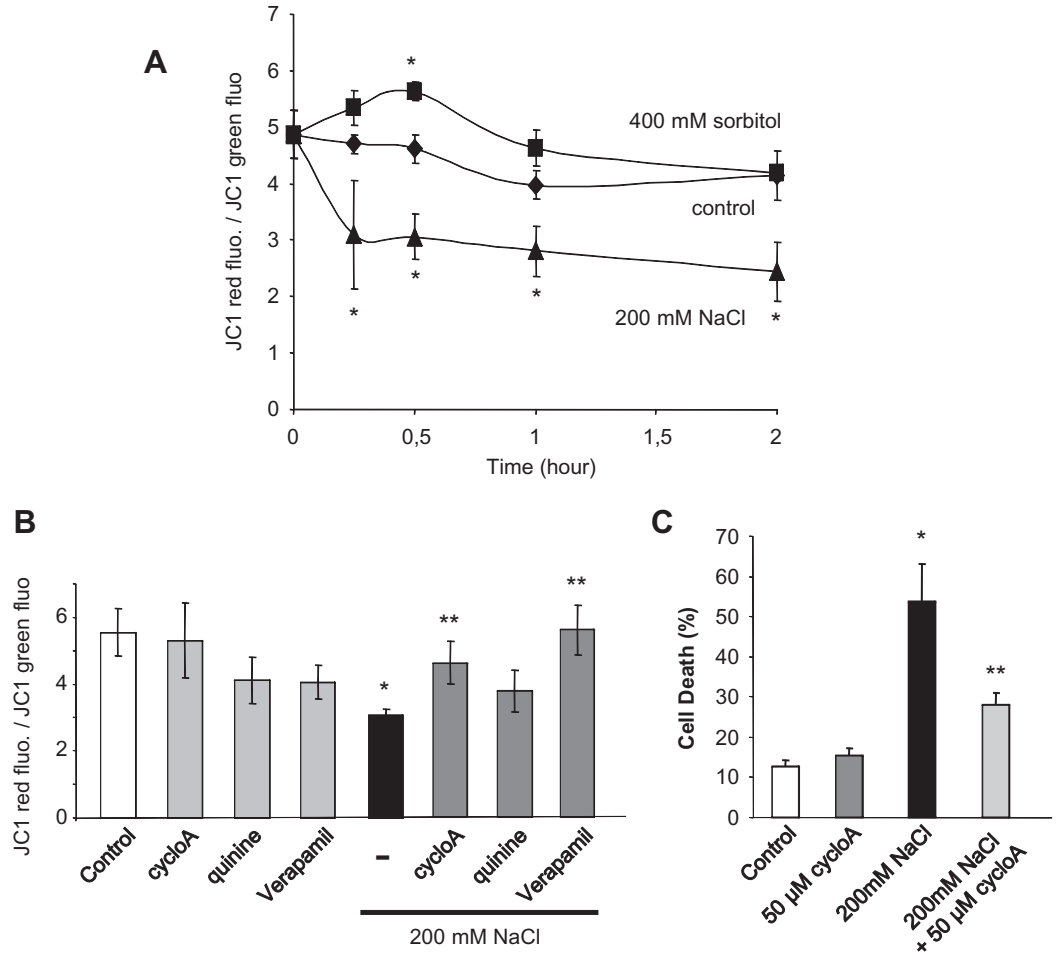

Fig. 7. (A) Variations of mitochondrial membrane potential ($\Delta\Psi_m$) of BY-2 tobacco cells after treatments with 200 mM NaCl or 400 mM sorbitol. (B) Effect of 50 µM cyclosporin A (CsA), an inhibitor of the permeability transition pore, 1 mM quinine, or 200 µM verapamil, inhibitors of NSCCs, on $\Delta\Psi_m$ variation induced by 200 mM NaCl after 15 min. The data reflect the means±SE of at least four independent experiments. (C) Effect of 50 µM CsA, 1 mM quinine, or 200 µM verapamil on cell death induced by 200 mM NaCl. The data reflect the means±SE of at least three independent replicates. *Significantly different from controls, $P < 0.05$; **significantly different from the NaCl-treated cells, $P < 0.05$.

Gd^{3+} but not by dantrolene and U73122, inhibitors of calcium-induced calcium release channels and of the inositol triphosphate receptor, respectively, known to be efficient in plants (Meimoun *et al.*, 2009). This suggests that the $[Ca^{2+}]_{cyt}$ increase was not due to Ca^{2+} release from intracellular Ca^{2+} stores, but to an influx through plasma membrane-permeable Ca^{2+} channels. Although rapid, the Ca^{2+} influxes happened after the $^1O_2$ generation since DABCO pre-treatments strongly decreased these influxes, suggesting that they were dependent on the generation of $^1O_2$. Accordingly, SHAM decreased the Ca^{2+} influxes to a lower extent and Tiron was unable to decrease them. This confirms the hypothesis that an $^1O_2$-dependent Ca^{2+} influx was induced by sorbitol and NaCl and highlights the role of $^1O_2$ as a signalling molecule (Fischer *et al.*, 2013).

Perturbation of Ca^{2+} homeostasis in plant cells, as well as in animal cells, has been described as a prerequisite for PCD (Grant *et al.*, 2000; Davis and Distelhorst, 2006; Lecourieux *et al.*, 2006). It was not possible to ascertain that in the BY-2 population all cells respond with a Ca^{2+} increase in the face of hyperosmotic stress. However, if only non-dying cells respond with a Ca^{2+} increase, this Ca^{2+} increase has no role in inducing PCD. In other words, if only dying cells (or even all cells) respond with a Ca^{2+} increase, since La^{3+} was inefficient in decreasing NaCl- and sorbitol-induced cell death, and even enhanced this cell death, it could suggest that Ca^{2+} influx could participate in cell protection. After perception of salt stress, the Ca^{2+} spike generated in the cytoplasm of root cells is known to activate the *S*alt *O*verly *S*ensitive (SOS) signal transduction cascade to protect the cells from damage due to excessive ion accumulation (Ji *et al.*, 2013). *SOS3* encodes a myristoylated calcium-binding protein that appears to function as a primary calcium sensor to perceive the increase in cytosolic Ca^{2+} triggered by Na^+ excess that has entered the cytoplasm. Upon binding to Ca^{2+}, SOS3 is able to interact with and activate the protein kinase SOS2 which phosphorylates SOS3 proteins. SOS3–SOS2 interactions recruit SOS2 to the plasma membrane, leading to activation of the downstream target SOS1, an Na^+/H^+ antiporter allowing extrusion of excessive Na^+ from the cytosol (Ji *et al.*, 2013). However, in

the present model, neither of these early linked events, Ca^{2+} increase and $^1O_2$, seemed to be involved in PCD.

On the other hand, Tiron, a scavenger of $O_2^{\cdot-}$, and DPI, an inhibitor of NADPH-oxidase, decreased the NaCl- and sorbitol-induced cell death and the delayed generation of ROS. This indicated that the delayed and more sustained $O_2^{\cdot-}$ generation from NADPH-oxidase activity could play a central role in the death of these cells. Several reports implicate NADPH-oxidase activity in production of ROS in salinity stress, with the ROS resulting in Ca^{2+} influx. In the present model, no effect of DPI on early stress-induced Ca^{2+} increase could be detected (Supplementary Fig. S2 available at *JXB* online), in accordance with the delayed DPI-sensitive ROS generation. However, from the present data, a delayed increase in Ca^{2+} linked to NADPH-oxidase activity cannot be excluded, but this increase in Ca^{2+} should be La^{3+} independent, since La^{3+} could not decrease cell death. It is obvious that sorbitol-induced ROS generation could not depend on Na^+ influx and thus possibly other hyperosmotic-induced events (e.g. NO production) could participate in NADPH-oxidase-dependent ROS generation observed in response to sorbitol and NaCl. However, upon NaCl stress, the delayed ROS generation could be decreased by quinine and verapamil, putative inhibitors of NSCCs (Demidchik *et al.*, 2002*a*, *b*). Even though no definitive molecular candidates have clearly emerged for NSCCs, it seems that various classes of NSCCs could be responsible for influx of Na^+ under salt stress, especially a depolarization-activated class of NSCCs (Demidchik and Maathuis, 2007). A rapid and large depolarization of the BY-2 cells could be recorded upon NaCl addition due to an increase in a current sensitive to quinine and verapamil but also to TEA^+, an inhibitor of K^+ channels known to block some NSCCs (Demidchik *et al.*, 2002*a*). It could also be verified that the accumulation of Na^+ in the cell was decreased upon pre-treatment with quinine or TEA^+, strongly suggesting that NSCCs were responsible for Na^+ influx into BY-2 cells. Moreover, these NSCC blockers were efficient in decreasing the NaCl-induced cell death, highlighting the toxic effect of Na^+ as previously reported (Huh *et al.*, 2002; Affenzeller *et al.*, 2009; Wang *et al.*, 2010). It is further noticeable that La^{3+}, a potent inhibitor of some NSCCs (Demidchick *et al.*, 2002*a*, *b*), was unable to decrease NaCl-induced cell death as well as the delayed ROS generation, whereas the NSCC blockers quinine, verapamil, and TEA^+ failed to decrease the NaCl-induced Ca^{2+} increase (Supplementary Fig. S3 available at JXB online). This indicates that the Ca^{2+} influx was completely dissociated from Na^+ influx through NSCCs. Moreover, sorbitol- and NaCl-induced Ca^{2+} influxes presented the same characteristics and were induced upon hyperpolarization in the case of sorbitol and depolarization in the case of NaCl, suggesting the voltage independence of the transporter involved. Further studies will be needed to determine if putative ligand-activated calcium channels such as cyclic nucleotide-gated channels or glutamate receptors could be responsible for these Ca^{2+} influxes in BY-2 cells; however, a putative candidate could be the calcium regulatory protein annexin (Laohavisit *et al.*, 2013).

Concerning ion flux regulation in response to sorbitol, a hyperpolarization of the BY-2 cells due to the decrease of anion currents was observed, as previously described in different models (Pennarun and Maillot, 1988; Teodoro *et al.*, 1998; Shabala *et al.*, 2000). Although such a regulation of anion current was shown to be involved during PCD induced by $HrpN_{ea}$, a hypersensitive elicitor from *Erwinia amylovora* (Reboutier *et al.* 2005), it did not seem to be involved in sorbitol-induced PCD since bromotetramisole, an activator of anion channels, failed to limit sorbitol-induced PCD (data

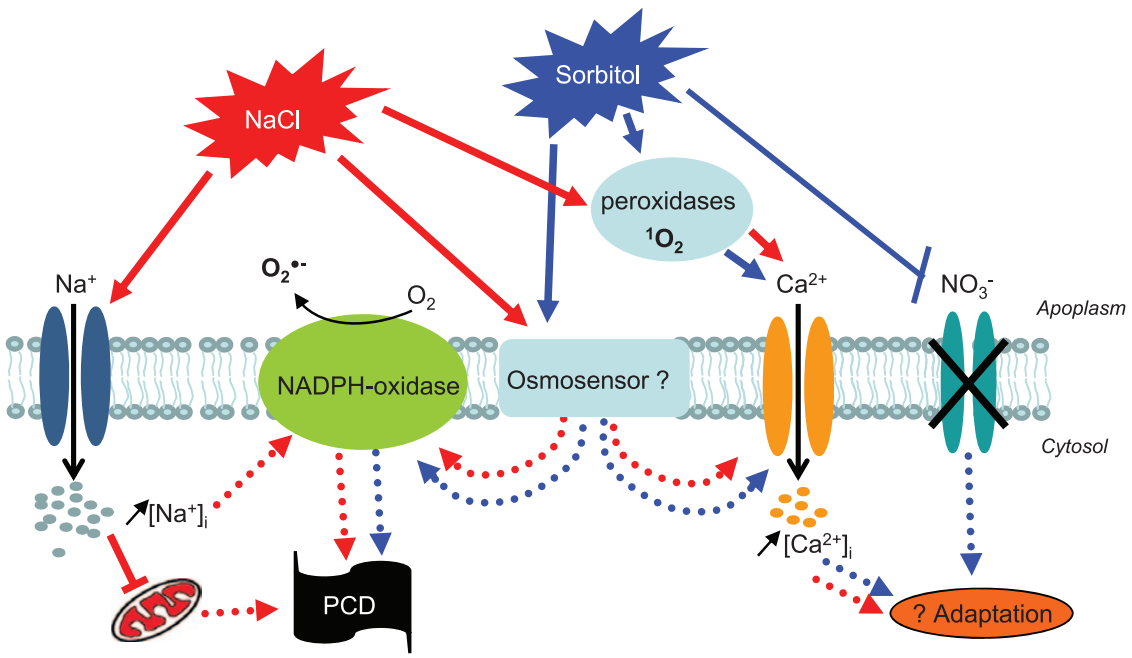

Fig. 8. Possible pathways induced by NaCl and sorbitol leading to cell death of tobacco cells. (This figure is available in colour at *JXB* online.)

not shown), in contrast to the previously observed effect of $HrpN_{ea}$ (Reboutier *et al.*, 2005).

Although ROS-activated outward-rectifying K^+ channels (KORCs) were shown to be involved in salt-induced PCD (Demidchik *et al.*, 2003, 2010), it was not possible to detect rapid activation of KORCs in response to NaCl or sorbitol. However, an activation of KORCs after addition of NaCl cannot be excluded, this current being masked in the large Na^+ current recorded. On the other hand, KORC activation could also be delayed, as was recently reported in response to O_3 (Tran *et al.*, 2013).

Finally, one of the most important differences observed between sorbitol- and NaCl-induced PCD in BY-2 cells was the role of mitochondria. Sorbitol did not affect mitochondrial polarization and even slightly and transiently stimulated its polarization, whereas NaCl induced a large mitochondrial depolarization. This depolarization was probably involved in the formation of the PTP since CsA, an inhibitor of PTP, could reduce the NaCl-induced decrease in $\Delta\Psi_m$ as previously described (Wang *et al.*, 2010) and also the NaCl-induced cell death. This could be related to observation made on *Micrasterias denticulate* (Affenzeller *et al.*, 2009) for which a typical laddering of the DNA was only observed for NaCl-stressed cells but not for sorbitol-treated cells. The endonuclease responsible for this laddering could be released from mitochondria through PTPs (Vianello *et al.*, 2007). It is to be noted that the inhibitors of NSCCs, verapamil, quinine, and TEA^+, were also efficient in limiting the loss in $\Delta\Psi_m$, suggesting a direct role for cytosolic Na^+-induced mitochondrial dysfunction.

As already described in numerous models, in BY-2 cells overlapping responses exist in response to ionic and non-ionic hyperosmotic stress and, among them, a PCD process. However, some overlapping responses such as the early transient $^1O_2$ generation responsible for an influx of Ca^{2+} did not seem to be involved in PCD progress, while other shared responses such as the delayed NADPH-oxidase stimulation were important for these processes (Fig. 8). Specific responses also seemed to be involved in the PCD processes since upon NaCl stress, NADPH-oxidase stimulation was at least partly due to Na^+ influx through NSCCs, which also seemed to be responsible for mitochondrial depolarization not observed after the sorbitol challenge. Further studies will be needed to characterize fully the pathways leading to PCD induced by these hyperosmotic stresses.

Supplementary data

Supplementary data are available at *JXB* online.

Figure S1. Typical anion current recorded in control conditions in BY-2 cells.

Figure S2. NaCl- and sorbitol-induced $[Ca^{2+}]_{cyt}$ increase in aequorin-expressing-tobacco BY-2 cells after a pre-treatment with the inhibitor of NADPH-oxidase DPI (20 μM).

Figure S3. NaCl-induced $[Ca^{2+}]_{cyt}$ increases in aequorin expressing-tobacco BY-2 cells after pre-treatments with the NSCC blockers quinine, verapamil, or TEA^+.

Acknowledgements

This research was partially supported by the Japan Society for the Promotion of Science, Grant-in-Aid for JSPS Fellows to TK. EM was supported by Fondo Giovani provided by the Ministry of Education, Universities and Research (MUIR). SM and EA were supported by the Future and Emerging Technologies (FET) programme within the 7th Framework Programme for Research of the European Commission, under FET-Open grant number 293431. We thank Christian Mazars (LRSV UPS CNRS, Toulouse, France) for the kind gift of the BY-2 aequorin cell line.

References

Affenzeller MJ, Darehshouri A, Andosch A, Lütz C, Lütz-Meindl U. 2009. Salt stress-induced cell death in the unicellular green alga *Micrasterias denticulata* Matthias. *Journal of Experimental Botany* **60,** 939–954.

Chen Z, Cuin TA, Zhou M, Twomey A, Naidu BP, Shabala S. 2007. Compatible solute accumulation and stress-mitigating effects in barley genotypes contrasting in their salt tolerance. *Journal of Experimental Botany* **58,** 4245–4255.

Davis MC, Distelhorst CW. 2006. Live free or die: an immature T cell decision encoded in distinct Bcl-2 sensitive and insensitive Ca^{2+} signals. *Cell Cycle* **5,** 1171–1174.

Demidchik V, Bowen HC, Maathuis FJ, Shabala SN, Tester MA, White PJ, Davies JM. 2002a. *Arabidopsis thaliana* root non-selective cation channels mediate calcium uptake and are involved in growth. *The Plant Journal* **32,** 799–808.

Demidchik V, Cuin TA, Svistunenko D, Smith SJ, Miller AJ, Shabala S, Sokolik A, Yurin V. 2010. Arabidopsis root K+-efflux conductance activated by hydroxyl radicals: single-channel properties, genetic basis and involvement in stress-induced cell death. *Journal of Cell Science* **123,** 1468–1479.

Demidchik V, Davenport RJ, Tester M. 2002b. Nonselective cation channels in plants. *Annual Review of Plant Biology* **53,** 67–107.

Demidchik V, Maathuis FJ. 2007. Physiological roles of nonselective cation channels in plants: from salt stress to signalling and development. *New Phytologist* **175,** 387–404.

Demidchik V, Tester M. 2002. Sodium fluxes through nonselective cation channels in the plasma membrane of protoplasts from Arabidopsis roots. *Plant Physiology* **128,** 379–387.

Donaldson L, Ludidib N, Knight MR, Gehring C, Denby K. 2004. Salt and osmotic stress cause rapid increases in *Arabidopsis thaliana* cGMP levels. *FEBS Letters* **569,** 317–320.

Duan Y, Zhang W, Li B, Wang Y, Li K, Sodmergen, Han C, Zhang Y, Li X. 2010. An endoplasmic reticulum response pathway mediates programmed cell death of root tip induced by water stress in *Arabidopsis*. *New Phytologist* **186,** 681–695.

Errakhi R, Meimoun P, Lehner A, Vidal G, Briand J, Corbineau F, Rona JP, Bouteau F. 2008. Anion channel activity is necessary to induce ethylene synthesis and programmed cell death in response to oxalic acid. *Journal of Experimental Botany* **59,** 3121–3129.

Finkel AS, Redman S. 1984. Theory and operation of a single microelectrode voltage clamp. *Journal of Neuroscience Methods* **11,** 101–127.

Fischer BB, Hideg E, Krieger-Liszkay A. 2013. Production, detection, and signaling of singlet oxygen in photosynthetic organisms. *Antioxidant and Redox Signaling* **18,** 2145–2162.

Galvez AS, Ulloa JA, Chiong M, Criollo A, Eisner V, Barros LF, Lavandero S. 2003. Aldose reductase induced by hyperosmotic stress mediates cardiomyocyte apoptosis: differential effet of sorbitol. *Journal of Biological Chemistry* **278,** 38484–38494.

Gauthier A, Lamotte O, Reboutier D, Bouteau F, Pugin A, Wendehenne D. 2007. Cryptogein-induced anion effluxes: electrophysiological properties and analysis of the mechanisms through which they contribute to the elicitor-triggered cell death. *Plant Signaling and Behavior* **2,** 89–98.

Grant M, Brown I, Adams S, Knight M, Ainslie A, Mansfield J. 2000. The RPM1 plant disease resistance gene facilitates a rapid and sustained increase in cytosolic calcium that is necessary for the oxidative burst and hypersensitive cell death. *The Plant Journal* **23,** 441–450.

Guo W, Ye Z, Wang G, Zhao X, Yuan J, Du Y. 2009. Measurement of oligochitosan–tobacco cell interaction by fluorometric method using europium complexes as fluorescence probes. *Talanta* **78,** 977–982.

Hossain MS, Ye W, Hossain MA, Okuma E, Uraji M, Nakamura Y, Mori IC, Murata Y. 2013. Glucosinolate degradation products, isothiocyanates, nitriles, and thiocyanates, induce stomatal closure accompanied by peroxidase-mediated reactive oxygen species production in *Arabidopsis thaliana*. *Bioscience Biotechnology Biochemistry* **77,** 977–983.

Hua JM, Wang XL, Zhai FQ, Yan F, Feng K. 2008. Effects of NaCl and Ca^{2+} on membrane potential of epidermal cells of maize roots. *Agricultural Science in China* **7,** 291–296.

Huh GH, Damsz B, Matsumoto TK, Reddy MP, Rus AM, Ibeas JI, Narasimhan ML, Bressan RA, Hasegawa PM. 2002. Salt causes ion disequilibrium-induced programmed cell death in yeast and plants. *The Plant Journal* **29,** 649–659.

Jacoby RP, Taylor NL, Millar AH. 2011. The role of mitochondrial respiration in salinity tolerance. *Trends in Plant Science* **16,** 614–623.

Ji H, Pardo JM, Batelli G, Van Oosten MJ, Bressan RA, Li X. 2013. The Salt Overly Sensitive (SOS) pathway: established and emerging roles. *Molecular Plant* **6,** 275–286.

Kadono T, Tran D, Errakhi R, Hiramatsu T, Meimoun P, Briand J, Iwaya-Inoue M, Kawano T, Bouteau F. 2010. Increased anion channel activity is an unavoidable event in ozone-induced programmed cell death. *PLoS One* **5,** e13373.

Kadono T, Yamaguchi Y, Furuichi T, Hirono M, Garrec JP, Kawano T. 2006. Ozone-induced cell death mediated with oxidative and calcium signaling pathways in tobacco Bel-W3 and Bel-B cell suspension cultures. *Plant Signaling and Behavior* **1,** 312–322.

Kanofsky JR. 2000. Assay for singlet-oxygen generation by peroxidases using 1270-nm chemiluminescence. *Methods in Enzymology* **319,** 59–67.

Kawano T, Sahashi N, Takahashi K, Uozumi N, Muto S. 1998. Salicylic acid induces extracellular superoxide generation followed by an increase in cytosolic calcium ion in tobacco suspension culture: the earliest events in salicylic acid signal transduction. *Plant and Cell Physiology* **39,** 721–730.

Kim BG, Waadt R, Cheong YH, Pandey GK, Dominguez-Solis JR, Schultke S, Lee SC, Kudla J, Luan S. 2007. The calcium sensor CBL10 mediates salt tolerance by regulating ion homeostasis in *Arabidopsis*. *The Plant Journal* **52,** 473–484.

Knight H, Trewavas AJ, Knight MR. 1996. Cold calcium signaling in *Arabidopsis* involves two cellular pools and a change in calcium signature after acclimation. *The Plant Cell* **8,** 489–503.

Knight H, Trewavas AJ, Knight MR. 1997. Calcium signalling in *Arabidopsis thaliana* responding to drought and salinity. *The Plant Journal* **12,** 1067–1078.

Krieger-Liszkay A. 2004. Singlet oxygen production in photosynthesis. *Journal of Experimental Botany* **56,** 337–346.

Laohavisit A, Richards SL, Shabala L, *et al*. 2013. Salinity-induced calcium signaling and root adaptation in *Arabidopsis* require the calcium regulatory protein annexin1. *Plant Physiology* **163,** 253–262.

Lecourieux D, Ranjeva R, Pugin A. 2006. Calcium in plant defence-signalling pathways. *New Phytologist* **171,** 249–269.

Li ZS, Delrot S. 1987. Osmotic dependence of the transmembrane potential difference of broadbean mesocarp cells. *Plant Physiology* **84,** 895–899.

Lin J, Wang Y, Wang G. 2006. Salt stress-induced programmed cell death in tobacco protoplasts is mediated by reactive oxygen species and mitochondrial permeability transition pore status. *Journal of Plant Physiology* **163,** 731–739.

Meimoun P, Vidal G, Bohrer AS, Lehner A, Tran D, Briand J, Bouteau F, Rona JP. 2009. Intracellular Ca^{2+} stores could participate to abscisic acid-induced depolarization and stomatal closure in *Arabidopsis thaliana*. *Plant Signaling and Behavior* **4,** 830–835.

Murata T, Goshima F, Yamauchi Y, Koshizuka T, Takakuwa H, Nishiyama Y. 2002. Herpes simplex virus type 2 US3 blocks apoptosis induced by sorbitol treatment. *Microbes and Infection* **4,** 707–712.

Nakano M, Sugioka K, Ushijima Y, Goto T. 1986. Chemiluminescence probe with *Cypridina* luciferin analog, 2-methyl-6-phenyl-3,7-dihydroimidazo[1,2-a]pyrazin-3-one, for estimating the ability of human-granulocytes to generate $O2^{-}$. *Analytical Biochemistry* **159,** 363–369

Niswander JM, Dokas LA. 2007. Hyperosmotic stress-induced caspase-3 activation is mediated by p38 MAPK in the hippocampus. *Brain Research* **1186,** 1–11.

Pandolfi C, Potossin I, Cuin T, Mancuso S, Shabala S. 2010. Specificity of polyamine effects on NaCl-induced ion flux kinetics and salt stress amelioration in plants. *Plant and Cell Physiology* **51,** 422–434.

Pauly N, Knight MR, Thuleau P, Graziana A, Muto S, Ranjeva R, Mazars C. 2001. The nucleus together with the cytosol generates patterns of specific cellular calcium signatures in tobacco suspension culture cells. *Cell Calcium* **30,** 413–421.

Parre E, Ghars MA, Leprince AS, Thiery L, Lefebvre D, Bordenave M, Richard L, Mazars C, Abdelly C, Savoure A. 2007. Calcium signaling via phospholipase C is essential for proline

accumulation upon ionic but not nonionic hyperosmotic stresses in *Arabidopsis*. *Plant Physiology* **144,** 503–512.

Pennarun AM, Maillot C. 1988. Cl^- flux responding to a turgor drop in cells of *Acer pseudoplatanus*. *Plant Physiology and Biochemistry* **26,** 117–124.

Ranf S, Wunnenberg P, Lee J, Becker D, Dunkel M, Hedrich R, Scheel D, Dietrich P. 2008. Loss of the vacuolar cation channel, *AtTPC1*, does not impair Ca^{2+} signals induced by abiotic and biotic stresses. *The Plant Journal* **53,** 287–299.

Reboutier D, Frankart C, Vedel R, Brault M, Duggleby RG, Rona JP, Barny MA, Bouteau F. 2005. A CFTR chloride channel activator prevents HrpN(ea)-induced cell death *in Arabidopsis thaliana* suspension cells. *Plant Physiology and Biochemistry* **43,** 567–572.

Shabala S. 2009. Salinity and programmed cell death: unravelling mechanisms for ion specific signalling. *Journal of Experimental Botany* **60,** 709–712.

Shabala S, Babourina O, Newman I. 2000. Ion-specific mechanisms of osmoregulation in bean mesophyll cells. *Journal of Experimental Botany* **51,** 1243–1253.

Shabala S, Cuin TA. 2008. Potassium transport and plant salt tolerance. *Physiologia Plantarum* **133,** 651–669.

Shabala SN, Lew RR. 2002. Turgor regulation in osmotically stressed *Arabidopsis* epidermal root cells. Direct support for the role of inorganic ion uptake as revealed by concurrent flux and cell turgor measurements. *Plant Physiology* **129,** 290–299.

Stief TW. 2003. The physiology and pharmacology of singlet oxygen. *Medical Hypotheses* **60,** 567–572.

Tarr M, Valenzeno DP. 2003. Singlet oxygen: the relevance of extracellular production mechanisms to oxidative stress *in vivo*. *Photochemical and Photobiological Sciences* **2,** 355–361.

Teodoro AE, Zingarelli L, Lado P. 1998. Early changes of Cl^- efflux and H^+ extrusion induced by osmotic stress in *Arabidopsis thaliana* cells. *Physiologia Plantarum* **102,** 29–37.

Tester M, Davenport R. 2003. Na^+ tolerance and Na^+ transport in higher plants. *Annals of Botany* **91,** 503–505.

Tran D, El-Maarouf-Bouteau H, Rossi M, Biligui B, Briand J, Kawano T, Mancuso S, Bouteau F. 2013. Post-transcriptional regulation of GORK channels by superoxide anion contributes to increases in outward-rectifying K^+ currents. *New Phytologist* **198,** 1039–1048.

Triantaphylidès C, Krischke M, Hoeberichts FA, Ksas B, Gresser G, Havaux M, Van Breusegem F, Mueller MJ. 2008. Singlet oxygen is the major reactive oxygen species involved in photooxidative damage to plants. *Plant Physiology* **148,** 960–968.

Tsiatsiani L, Van Breusegem F, Gallois P, Zavialov A, Lam E, Bozhkov PV. 2011. Metacaspases. *Cell Death and Differentiation* **18,** 1279–1288.

van Doorn WG. 2011. Classes of programmed cell death in plants, compared to those in animals. *Journal of Experimental Botany* **62,** 4749–4761.

van Doorn WG, Beers EP, Dangl JL, *et al*. 2011. Morphological classification of plant cell deaths. *Cell Death and Differentiation* **18,** 1241–1246.

Vianello A, Zancani M, Peresson C, Petrussa E, Casolo V, Krajňáková J, Patui S, Braidot E, Macrì F. 2007. Plant mitochondrial pathway leading to programmed cell death. *Physiologia Plantarum* **129,** 242–252.

Wang J, Li X, Liu Y, Zhao X. 2010. Salt stress induces programmed cell death in *Thellungiella halophila* suspension-cultured cells. *Journal of Plant Physiology* **167,** 1145–1151.

Wegner LH, Stefano G, Shabala L, Rossi M, Mancuso S, Shabala S. 2011. Sequential depolarization of root cortical and stelar cells induced by an acute salt shock—implications for Na(+) and K(+) transport into xylem vessels. *Plant, Cell and Environment* **34,** 859–869.

Xiong L, Schumaker KS, Zhu JK. 2002. Cell signaling during cold, drought, and salt stress. *The Plant Cell* **14,** S165–S183.

Zhang B, Liu K, Zheng Y, Wang Y, Wang J, Liao H. 2013. Disruption of AtWNK8 enhances tolerance of *Arabidopsis* to salt and osmotic stresses via modulating proline content and activities of catalase and peroxidase. *International Journal of Molecular Sciences* **14,** 7032–7047.

Zingarelli L, Marre MT, Massardi F, Lado P. 1999. Effects of hyperosmotic stress on K^+ fluxes, H^+ extrusion, transmembrane electric potential difference and comparison with the effects of fusicoccin. *Physiologia Plantarum* **106,** 287–295.

Zhu JK. 2001. Plant salt tolerance. *Trends in Plant Science* **6,** 66–71.